Applications of Mathematics

Eric Lindström; Larisa Beilina

Energy norm error estimates and convergence analysis for a stabilized Maxwell's equations in conductive media

Applications of Mathematics, Vol. 69 (2024), No. 4, 415–436

Persistent URL: http://dml.cz/dmlcz/152526

Terms of use:

© Institute of Mathematics AS CR, 2024

Institute of Mathematics of the Czech Academy of Sciences provides access to digitized documents strictly for personal use. Each copy of any part of this document must contain these *Terms of use*.



This document has been digitized, optimized for electronic delivery and stamped with digital signature within the project *DML-CZ: The Czech Digital Mathematics Library* http://dml.cz

69 (2024) APPLICATIONS OF MATHEMATICS No. 4, 415–436

ENERGY NORM ERROR ESTIMATES AND CONVERGENCE ANALYSIS FOR A STABILIZED MAXWELL'S EQUATIONS IN CONDUCTIVE MEDIA

Eric Lindström, Larisa Beilina, Gothenburg

Received December 29, 2023. Published online May 27, 2024.

Abstract. The aim of this article is to investigate the well-posedness, stability of solutions to the time-dependent Maxwell's equations for electric field in conductive media in continuous and discrete settings, and study convergence analysis of the employed numerical scheme. The situation we consider would represent a physical problem where a subdomain is emerged in a homogeneous medium, characterized by constant dielectric permittivity and conductivity functions. It is well known that in these homogeneous regions the solution to the Maxwell's equations also solves the wave equation, which makes computations very efficient. In this way our problem can be considered as a coupling problem, for which we derive stability and convergence analysis. A number of numerical examples validate theoretical convergence rates of the proposed stabilized explicit finite element scheme.

Keywords: Maxwell's equation; finite element method; stability; a priori error analysis; energy error estimate; convergence analysis

MSC 2020: 65N15, 65N21, 65N30, 35Q61

1. Introduction

In this paper we consider the time-dependent Maxwell's equations in a bounded, simply connected spatial domain Ω. This domain is divided into two subdomains, the outer one, where the dielectric permittivity and conductivity are constant functions, and inner one, where they are allowed to vary but are still bounded functions.

One important (and of special interest for the authors) consequence of the results developed in this paper is the application of Maxwell's equations to solutions of *Coefficient Inverse Problems* (CIPs) [10]. In [41], [42] one can read about inverse

The research of both authors is supported by the Swedish Research Council grant VR 2018-03661. Open access funding provided by University of Gothenburg.

DOI: 10.21136/AM.2024.0248-23

© The author(s) 2024.

problems applied to imaging of buried objects, and in [12], [11], [35], inverse problems are used for medical imaging. In the latter case the problem is to reconstruct the dielectric permittivity and conductivity functions of an anatomically realistic phantom of a breast tissue. The dielectric properties of different tissue types in a breast are experimentally measured and known [34], but their distribution inside every particular breast tissue is unknown. Such a scenario is one case, where the domain decomposition can be a useful tool for solving the electromagnetic CIPs when the goal is determination of dielectric properties of the object from boundary measurements of the scattered electric field.

Under certain circumstances, it is known that the solution to the Maxwell's equations also solves the wave equation, which is widely studied, see [4], [3], [8], [12], [13]. In [13], a finite element analysis shows stability and consistency of the stabilized finite element method for the solution of Maxwell's equations in non-conductive media, and in [4] authors investigated a stabilized domain decomposition finite element method for the time harmonic Maxwell's equations. Stability and convergence analysis of a Domain Decomposition FE/FD method for time-dependent Maxwell's equations was presented in [3]. In our knowledge, all previously cited works consider non-conductive media, and the research concerning time-dependent Maxwell's equation for electric field in conductive media, where both dielectric permittivity and conductivity are space-dependent functions, is missing.

The stability and well-posedness of the wave equation are well understood and studied, see, e.g., [24], [31]. Certain model of wave equations have also been used to model inverse problems, see [10], [7], [25]. The progression to Maxwell's equations is arguably natural, since the system has wave-like structure. However, some complications occur from the presence of the double curl operator [33], [36]. Another theoretical complication is that when one analyzes the corresponding bilinear form induced by the variational form, one can see that it is not coercive [33], [36]. The coercivity is essential in proofs concerning the existence and uniqueness of solutions. The additional novelty of the presented work is in how we deal with coercivity of the bilinear form. Due to the fact that the bilinear form with presence of time-dependent terms turns out to be non-coercive, we split it and separate terms with derivatives in time in order to derive the coercivity for the remaining spatial part of the bilinear form using some minor restrictions on the gradient of the permittivity function. Then we use coercivity of the spatial part of the bilinear form in the proof of a priori error estimate. Derivation of quasi-coercivity of the entire scheme is a topic of an ongoing research.

To align the results with implementations of $P1$-methods, we introduce a slightly modified, stabilized problem. Otherwise, these methods would lead to spurious solutions (see [5], [8], [16], [17], [26], [27], [28], [29], [38], [40]) and it is well-known that

theoretically, divergence-free edge elements are a better fit, see [18], [23], [36], [37], [39]. More on various numerical methods for Maxwell equations and more details about the complications can be found in [1], [5], [4], [14], [19], [20], [23], [21], [33], [36], [38] and the references therein. Naturally, the theoretical results of this work are basis for numerical implementations, therefore we also present analysis of the corresponding discrete problem to our original model.

An outline of this paper is as follows. In Section 2 we introduce the mathematical model and present the stabilized problem for the time-dependent Maxwell's equations in conductive media. In Section 3 we state the variational problem for the stabilized model and formulate the finite element scheme. Section 4 is devoted to the energy norm error analysis and Section 5 presents derivation of a priori error estimates. In Section 6 we present numerical convergence tests verifying the theoretical results of this paper. Finally, in Section 7 we conclude the results of the paper.

2. The mathematical model

Consider the initial value problem for the electric field $E(x,t) = (E_1, E_2, E_3)(x,t)$, $x \in \mathbb{R}^3$, $t \in [0,T]$, for time-dependent Maxwell's equations in conductive media, under the assumptions that the dimensionless relative magnetic permeability of the medium is $\mu_r \equiv 1$:

$$\begin{gathered} \frac{1}{c^2}\varepsilon_r(x)\frac{\partial^2 E}{\partial t^2} + \nabla \times \nabla \times E = -\mu_0\sigma(x)\frac{\partial E}{\partial t} - j, \\ \nabla \cdot (\varepsilon E) = 0, \\ E(x,0) = f_0(x), \quad \frac{\partial E}{\partial t}(x,0) = f_1(x), \quad x \in \mathbb{R}^3,\ t \in (0,T]. \end{gathered} \tag{2.1}$$

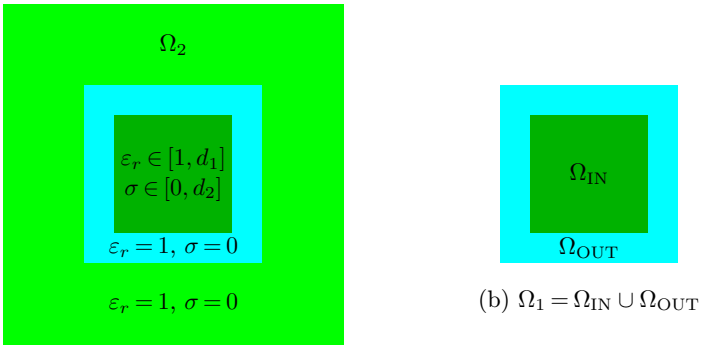
Here, $\varepsilon_r(x) = \varepsilon(x)/\varepsilon_0$ is the dimensionless relative dielectric permittivity, $\sigma(x)$ is the electric conductivity function; ε_0 and μ_0 are the permittivity and permeability of the free space, respectively, and $c = 1/\sqrt{\varepsilon_0\mu_0}$ is the speed of light in free space, and finally j is a given source function.

To solve problem (2.1) numerically, we consider it in a bounded simply connected spatial domain $\Omega \subset \mathbb{R}^n$, $n = 2, 3$ with boundary Γ, and time interval $J = (0,T)$. In this work we will study problem (2.1) in a special framework: we decompose the space domain Ω into two subdomains Ω_1 and Ω_2 such that $\Omega = \Omega_1 \cup \Omega_2$, $\Omega_1 \subset \Omega$. Additionally, the space domain Ω_1 is divided into two subdomains Ω_{IN} and Ω_{OUT} such that $\Omega_1 = \Omega_{\mathrm{IN}} \cup \Omega_{\mathrm{OUT}}$. Figure 1 illustrates domain decomposition of Ω. We assume that for some known constants $d_1 > 1$, $d_2 > 0$ chosen so that $d_1 > d_2$, the

functions $\varepsilon, \sigma \in C^2(\Omega) \cap L^\infty(\Omega)$ satisfy the following conditions:

$$\begin{aligned} &\varepsilon_r(x) \in [1, d_1], \quad \sigma(x) \in [0, d_2] \quad \text{for } x \in \Omega_{\text{IN}}, \\ &\varepsilon_r(x) = 1, \quad \sigma(x) = 0 \quad \text{for } x \in \Omega_2 \cup \Omega_{\text{OUT}}. \end{aligned} \tag{2.2}$$

We refer to [12] and references therein for justification and possible choice of these coefficients. Note also that we will only consider the relative permittivity from here on, and will therefore omit the index r in ε_r.



(a) $\Omega = \Omega_1 \cup \Omega_2$

(b) $\Omega_1 = \Omega_{\text{IN}} \cup \Omega_{\text{OUT}}$

Figure 1. The functions ε_r, σ in the domain decomposition of $\Omega = \Omega_1 \cup \Omega_2$ (left figure) such that $\Omega_1 = \Omega_{\text{IN}} \cup \Omega_{\text{OUT}}$ (middle figure).

We observe that conditions (2.2) on ε and σ together with the relation

$$\nabla \times \nabla \times E = \nabla(\nabla \cdot E) - \nabla \cdot (\nabla E), \tag{2.3}$$

and divergence-free condition $\nabla \cdot (\varepsilon E) = 0$ in Ω_2, make equations in (2.1) independent of each other in Ω_2 such that in Ω_2, we solve the system of uncoupled wave equations:

$$\frac{\partial^2 E}{\partial t^2} - \Delta E = 0, \quad (x, t) \in \Omega_2 \times (0, T]. \tag{2.4}$$

In [13], a finite element analysis shows stability and consistency of the stabilized finite element method for the solution of (2.1) with $\sigma(x) = 0$. In [4] a stabilized linear, domain decomposition, finite element method for the time harmonic Maxwell's equations was studied. In the current study we show stability and convergence analysis of the finite element method for solution of (2.1) under condition (2.2) on ε and σ.

Let $\Omega_T = \Omega \times (0, T)$, $\Gamma_T = \Gamma \times (0, T)$. Let us introduce the following spaces of real-valued functions:

$$\begin{aligned} H_E^2(\Omega_T) &:= \Big\{ w \in H^2(\Omega_T) \colon\ w(\cdot, 0) = f_0, \frac{\partial w}{\partial t}(\cdot, 0) = f_1 \Big\}, \\ H_E^1(\Omega_T) &:= \Big\{ w \in H^1(\Omega_T) \colon\ w(\cdot, 0) = f_0, \frac{\partial w}{\partial t}(\cdot, 0) = f_1 \Big\}. \end{aligned} \tag{2.5}$$

In this paper we study the following stabilized initial boundary value problem setting $\mathbf{H}^2_E(\Omega_T) = [H^2_E(\Omega_T)]^3$: find $E \in \mathbf{H}^2_E(\Omega_T)$ such that

$$\begin{cases} \varepsilon \dfrac{\partial^2 E}{\partial t^2} - \triangle E - \nabla(\nabla \cdot ((\varepsilon - 1)E)) = -\sigma(x)\dfrac{\partial E}{\partial t} - j & \text{in } \Omega_T, \\ E(\cdot, 0) = f_0(\cdot), \text{ and } \partial_t E(\cdot, 0) = f_1(\cdot) & \text{in } \Omega, \\ E = 0 & \text{on } \Gamma_T. \end{cases} \tag{2.6}$$

Here, the divergence-free condition $\nabla \cdot (\varepsilon E) = 0$ is hidden in the first equation of system (2.6).

3. Finite element discretization

Throughout the paper we denote the inner product in $[L^2(\Omega)]^d$, $d \in \{1, 2, 3\}$, by $(\cdot, \cdot)$, and the corresponding norm by $\|\cdot\|$.

Let us define the following L^2 scalar products used in the analysis:

$$\begin{aligned} (u, v) := (u, v)_\Omega = \int_\Omega uv \,\mathrm{d}\mathbf{x}, \quad ((u, v)) := ((u, v))_{\Omega_T} = \int_0^T \int_\Omega uv \,\mathrm{d}\mathbf{x}\,\mathrm{d}t, \\ \langle u, v\rangle := \langle u, v\rangle_\Gamma = \int_\Gamma uv \,\mathrm{d}\sigma, \quad \langle\langle u, v\rangle\rangle := \langle\langle u, v\rangle\rangle_{\Gamma_T} = \int_0^T \int_\Gamma uv \,\mathrm{d}\sigma\,\mathrm{d}t. \end{aligned} \tag{3.1}$$

Additionally, we define the ω-weighted $L^2(\Omega)$ norm

$$\|u\|_\omega := \sqrt{\int_\Omega \omega |u|^2 \,\mathrm{d}\mathbf{x}}, \quad \omega > 0,\ \omega \in L^\infty(\Omega), \tag{3.2}$$

together with the ω-weighted L^2 scalar product:

$$(u, v)_\omega := \int_\Omega \omega uv \,\mathrm{d}\mathbf{x}. \tag{3.3}$$

To formulate a finite element scheme for the model problem (2.6) in whole Ω, we discretize $\Omega_T = \Omega \times (0, T)$ using partition $K_h = \{K\}$ of $\overline{\Omega}$ into elements K, where $h = h(x)$ is a mesh function defined as $h = \max\limits_{K \in K_h} h_K$, where h_K denotes the local diameter of the element K. We also denote by $\partial K_h = \{\partial K\}$ a partition into boundaries ∂K of the elements K. Let J_τ be a uniform partition of the time interval $(0, T)$ into N subintervals $J = (t_{k-1}, t_k]$ with the time step $\tau = T/N$. We also assume a minimal angle condition on elements K in K_h, see [2], [32].

To formulate the finite element method for the spatial semi-discrete problem (2.6) in $\overline{\Omega}$ we introduce the finite element space $W_h^E(\overline{\Omega})$ for every component of the electric field E defined by

$$W_h^E(\overline{\Omega}) := \{w \in H^1(\overline{\Omega})\colon\ w|_K \in P_1(K)\ \forall\, K \in K_h\},$$

where $P_1(K)$ denotes the set of piecewise-linear functions on K. We define f_{0h}, f_{1h}, j_h to be the usual interpolants of f_0, f_1 and j, respectively, in (2.6) onto $[W_h^E(\overline{\Omega})]^3$.

Setting $\mathbf{W}^E(\Omega) = [W^E(\Omega)]^3$ and $\mathbf{W}_h^E(\overline{\Omega}) = [W_h^E(\overline{\Omega})]^3$, where the test function space is chosen as

$$\mathbf{W}_{h,0}^E(\overline{\Omega}) := \{\mathbf{v} \in \mathbf{W}_h^E(\overline{\Omega})\colon\ \mathbf{v} = 0 \text{ on } \Gamma\}, \tag{3.4}$$

the spatial semi-discrete problem (2.6) in $\overline{\Omega}$ reads:

Find $E_h \in \mathbf{W}_h^E(\overline{\Omega})$ *such that for all* $\mathbf{v} \in \mathbf{W}_{h,0}^E(\overline{\Omega})$,

$$\begin{aligned} B(E_h, \mathbf{v}) := (\varepsilon \partial_{tt} E_h, \mathbf{v}) + (\sigma \partial_t E_h, \mathbf{v}) + a(E_h, \mathbf{v}) = -(j, \mathbf{v}), \\ E_h(\cdot, 0) = f_{0h}(\cdot), \\ \partial_t E_h(\cdot, 0) = f_{1h}(\cdot) \quad \text{in } \overline{\Omega}. \end{aligned} \tag{3.5}$$

Here, a is a bilinear form defined as

$$a(E_h, \mathbf{v}) := (\nabla E_h, \nabla \mathbf{v}) + (\nabla\cdot((\varepsilon - 1)E_h), \nabla\cdot\mathbf{v}) - (n\cdot\nabla\cdot((\varepsilon - 1)E_h), \nabla\cdot\mathbf{v})_{\partial\Omega} - \langle \partial_n E_h, \mathbf{v}\rangle_\Gamma. \tag{3.6}$$

We observe that boundary terms in (3.6) disappear because of the definition of test space (3.4). Thus, the bilinear form (3.6) for the case of test space (3.4) will be transformed to

$$a(E_h, \mathbf{v}) := (\nabla E_h, \nabla \mathbf{v}) + (\nabla \cdot ((\varepsilon - 1)E_h), \nabla \cdot \mathbf{v}). \tag{3.7}$$

Let us recall the explicit fully discrete finite element scheme for solution of (3.5) for $k = 1, 2, \ldots, N-1$ and for all $\mathbf{v} \in \mathbf{W}_{h,0}^E(\overline{\Omega})$, which was derived in [11]:

$$\begin{aligned} \Big(\varepsilon_h \frac{E_h^{k+1} - 2E_h^k + E_h^{k-1}}{\tau^2}, \mathbf{v}\Big) + (\nabla E_h^k, \nabla \mathbf{v}) + (\nabla \cdot (\varepsilon_h E_h^k), \nabla \cdot \mathbf{v}) - (\nabla \cdot E_h^k, \nabla \cdot \mathbf{v}) \\ + \Big(\sigma_h \frac{E_h^{k+1} - E_h^{k-1}}{2\tau}, \mathbf{v}\Big) + (j_h^k, \mathbf{v}) = 0, \end{aligned} \tag{3.8}$$

$$E_h{}^0 = f_{0h} \quad \text{and} \quad E_h{}^1 = E_h{}^0 + \tau f_{1h} \quad \text{in } \overline{\Omega}.$$

In scheme (3.8) we denoted $E_h(k\tau)$ and $j_h(k\tau)$ by E_h^k and j_h^k, respectively, for $k = 1, 2, \ldots, N$. Rearranging the terms in (3.8) we get for $k = 1, 2, \ldots, N-1$, and for all $\mathbf{v} \in \mathbf{W}_{h,0}^E(\overline{\Omega})$,

(3.9)
$$\Big(\Big(\varepsilon_h + \frac{\tau}{2}\sigma_h\Big)E_h^{k+1}, \mathbf{v}\Big) = (2\varepsilon_h E_h^k, \mathbf{v}) - (\varepsilon_h E_h^{k-1}, \mathbf{v}) - \tau^2(\nabla E_h^k, \nabla \mathbf{v}) - \tau^2(\nabla \cdot (\varepsilon_h E_h^k), \nabla \cdot \mathbf{v}) + \tau^2(\nabla \cdot E_h^k, \nabla \cdot \mathbf{v}) + \tau\Big(\frac{\sigma_h}{2}E_h^{k-1}, \mathbf{v}\Big) - \tau^2(j_h^k, v),$$
$$E_h^0 = f_{0h} \quad \text{and} \quad E_h^1 = E_h^0 + \tau f_{1h} \quad \text{in } \overline{\Omega}.$$

For the convergence of this scheme the following CFL condition derived in [13] for the case of $\sigma = 0$ needs to hold:

$$\tau \leqslant \frac{h}{\eta}, \quad \eta = C\sqrt{1 + 3\|\varepsilon - 1\|_\infty}, \tag{3.10}$$

where C is a mesh independent constant. The CFL condition for the case when both functions $\varepsilon \neq 0$, $\sigma \neq 0$ is a topic of an ongoing research.

4. Energy norm error estimate (stability estimate)

In this section we first give a proof of energy estimate for the vector $E \in H^2(\Omega_T)$ of the continuous model problem (2.6). Then we formulate the stability estimate for semi-discrete problem, which is a consequence of the energy estimate for the continuous problem.

Theorem 4.1. *Assume that conditions* (2.2) *on the functions* $\varepsilon(x)$, $\sigma(x)$ *hold true. Let* $\Omega \subset \mathbb{R}^3$ *be a bounded domain with the piecewise smooth boundary* $\partial\Omega$. *For any* $t^* \in (0, T)$ *let* $\Omega_{t^*} = \Omega \times (0, t^*)$ *and* $\Gamma_{t^*} = \Gamma \times (0, t^*)$. *Suppose that there exists a solution* $E \in H^2(\Omega_T)$ *of the model problem* (2.6). *Then the vector* E *is unique and there exists a constant* $C = C(\|\varepsilon\|_{C^2(\Omega)}, \|\sigma\|, t^*)$ *such that the following energy estimate holds true for all* $\varepsilon \geqslant 1$ *in* (2.6) *satisfying condition* (5.10)*:*

$$\begin{aligned} |\!|\!| E |\!|\!|^2(t^*) &:= \|\partial_t E\|_\varepsilon^2(t^*) + \|E\|_\sigma^2(t^*) + \|\nabla E\|^2(t^*) + \|\nabla \cdot E\|_{\varepsilon-1}^2(t^*) \\ &\leqslant C[\|j\|_{\Omega_{t^*}}^2 + \|f_1\|_\varepsilon^2 + \|\nabla f_0\|^2 + \|f_0\|_\sigma^2 + \|\nabla \cdot f_0\|_{\varepsilon-1}^2]. \end{aligned} \tag{4.1}$$

P r o o f. To simplify notation in our proof we denote the terms in the first line of (2.6) as

$$\underbrace{\varepsilon\partial_{tt}E}_{\mathbf{I}_1}\underbrace{-\Delta E}_{\mathbf{I}_2} + \underbrace{\nabla(\nabla \cdot ((1-\varepsilon)E)}_{\mathbf{I}_3} = \underbrace{-\sigma\partial_t E}_{\mathbf{I}_4} - \underbrace{j}_{\mathbf{I}_5}, \tag{4.2}$$

i.e., $\mathbf{I}_1 + \mathbf{I}_2 + \mathbf{I}_3 = \mathbf{I}_4 + \mathbf{I}_5$.

Through the proof we denote a generic constant of moderate size by $C := C(\|\varepsilon - 1\|_{\mathrm{C}^2(\Omega)}, \|\sigma\|_\infty, t^*)$. To prove the energy estimate we multiply (4.2) by $2\partial_t E$, integrate over Ω_{t^*}, and study each term separately. For the first term in (4.2) we have

(4.3)
$$((\mathbf{I}_1, 2\partial_t E))_{\Omega_{t^*}} = ((2\partial_{tt} E, \partial_t E))_{\varepsilon,\Omega_{t^*}} = \int_0^{t^*} \partial_t \|\partial_t E\|_\varepsilon^2(t)\,\mathrm{d}t = \|\partial_t E\|_\varepsilon^2(t^*) - \|f_1\|_\varepsilon^2,$$

where we used the chain rule, fundamental theorem of calculus and boundary conditions of (2.6).

Next we have that

(4.4)
$$\begin{aligned}((\mathbf{I}_2, 2\partial_t E))_{\Omega_{t^*}} &= -((\Delta E, 2\partial_t E))_{\Omega_{t^*}} \\ &= -2\langle\langle \partial_n E, \partial_t E\rangle\rangle_{\Gamma_{t^*}} + ((2\nabla E, \nabla(\partial_t E)))_{\Omega_{t^*}} \\ &= \int_0^{t^*} \partial_t \|\nabla E\|^2(t)\,\mathrm{d}t = \|\nabla E\|^2(t^*) - \|\nabla f_0\|^2,\end{aligned}$$

where we use spatial integration by parts, boundary condition $E = 0$ such that $\|\partial_t E\|_{\Gamma_t^*} = 0$.

For the third term in (4.2) we integrate by parts spatially twice and get

(4.5)
$$\begin{aligned}((\mathbf{I}_3, 2\partial_t E))_{\Omega_{t^*}} &= ((\nabla(\nabla\cdot((1-\varepsilon)E), 2\partial_t E))_{\Omega_{t^*}} \\ &= 2\langle\langle n\cdot(\nabla\cdot((1-\varepsilon)E), \partial_t E\rangle\rangle_{\Gamma_{t^*}} - 2((\nabla\cdot((1-\varepsilon)E), \nabla\cdot\partial_t E))_{\Omega_{t^*}} \\ &= -2((\nabla(1-\varepsilon)\cdot E, \nabla\cdot\partial_t E))_{\Omega_{t^*}} + ((2\nabla\cdot E, \nabla\cdot\partial_t E))_{\varepsilon-1,\Omega_{t^*}} \\ &= -2\langle\langle \nabla(1-\varepsilon)\cdot E, n\cdot\partial_t E\rangle\rangle_{\Gamma_{t^*}} + 2((\nabla(\nabla(1-\varepsilon)\cdot E), \partial_t E))_{\Omega_{t^*}} \\ &\quad + \int_0^{t^*} \partial_t \|\nabla\cdot E\|_{\varepsilon-1}^2(t)\,\mathrm{d}t \\ &= 2((\nabla(\nabla(1-\varepsilon)\cdot E), \partial_t E))_{\Omega_{t^*}} + \|\nabla\cdot E\|_{\varepsilon-1}^2(t^*) - \|\nabla\cdot f_0\|_{\varepsilon-1}^2.\end{aligned}$$

Above, we made use of (2.2) (note that since $\varepsilon \equiv 1$ on a neighbourhood of Γ, we have $(1-\varepsilon)|_\Gamma \equiv 0$ and $\nabla(1-\varepsilon)|_\Gamma \equiv 0$). We also made use of the fact that $\nabla\cdot((1-\varepsilon)E) = \nabla(1-\varepsilon)E + (1-\varepsilon)\nabla\cdot E$.

Before estimating the fourth term in (4.2) we first note that

$$E(x,t^*) = E(x,0) + \int_0^{t^*} \partial_t E(x,t)\,\mathrm{d}t,$$

and using that $(a+b)^2 \leqslant 2a^2 + 2b^2$ we get

(4.6)
$$E^2(x,t^*) \leqslant 2E^2(x,0) + 2\left(\int_0^{t^*} \partial_t E(x,t)\,\mathrm{d}t\right)^2 \leqslant 2E^2(x,0) + 2\int_0^{t^*} (\partial_t E)^2(x,t)\,\mathrm{d}t.$$

Integrating (4.6) over Ω, we arrive at

$$-2((\partial_t E, \partial_t E))_{\Omega_{t^*}} \leqslant -\|E\|^2(t^*) + 2\|E\|^2(0) = -\|E\|^2(t^*) + 2\|f_0\|^2.$$

Applying this to our case, we have that

$$((\mathbf{I}_4, 2\partial_t E))_{\Omega_{t^*}} = -2((\partial_t E, \partial_t E))_{\sigma,\Omega_{t^*}} \leqslant -\|E\|^2_\sigma(t^*) + 2\|f_0\|^2_\sigma. \tag{4.7}$$

For our final term in (4.2), we simply use that $2ab \leqslant a^2 + b^2$:

$$((\mathbf{I}_5, 2\partial_t E))_{\Omega_{t^*}} \leqslant ((|j|, 2|\partial_t E|))_{\Omega_{t^*}} \leqslant \|j\|^2_{\Omega_{t^*}} + \|\partial_t E\|^2_{\Omega_{t^*}}. \tag{4.8}$$

Next we collect all the terms (4.3)–(4.8) to arrive at

$$\begin{aligned} \|\partial_t E\|^2_\varepsilon(t^*) + \|\nabla E\|^2(t^*) + \|\nabla \cdot E\|^2_{\varepsilon-1}(t^*) + \|E\|^2_\sigma(t^*) \\ \leqslant \|f_1\|^2_\varepsilon + \|\nabla f_0\|^2 + \|\nabla \cdot f_0\|^2_{\varepsilon-1} + 2\|f_0\|^2_\sigma + \|j\|^2_{\Omega_{t^*}} \\ + \|\partial_t E\|^2_{\Omega_{t^*}} + 2((\nabla(\nabla(\varepsilon - 1) \cdot E), \partial_t E))_{\Omega_{t^*}}. \end{aligned} \tag{4.9}$$

We may estimate the last term of (4.9) using condition (5.10) such that

$$|\nabla(\nabla(\varepsilon - 1) \cdot E)| \leqslant C(|E| + |\nabla E|).$$

Thus, the above estimate together with the inequality $ab \leqslant a^2/2 + b^2/2$ yields

$$\begin{aligned} 2((|\nabla(\nabla(\varepsilon - 1) \cdot E)|, |\partial_t E|))_{\Omega_{t^*}} &\leqslant 2C((|E| + |\nabla E|, |\partial_t E|))_{\Omega_{t^*}} \\ &\leqslant C(\|(|E| + |\nabla E|)\|^2_{\Omega_{t^*}} + \|\partial_t E\|^2_{\Omega_{t^*}}) \\ &\leqslant C(\|E\|^2_{\Omega_{t^*}} + \|\nabla E\|^2_{\Omega_{t^*}} + \|\partial_t E\|^2_{\Omega_{t^*}}). \end{aligned}$$

Now we can rewrite (4.9) as

$$\begin{aligned} F(t^*) &\leqslant g(t^*) + C(\|\partial_t E\|^2_{\Omega_{t^*}} + \|\nabla E\|^2_{\Omega_{t^*}} + \|E\|^2_{\Omega_{t^*}}) \\ &\leqslant g(t^*) + C(\|\partial_t E\|^2_{\varepsilon,\Omega_{t^*}} + \|\nabla E\|^2_{\Omega_{t^*}} + \|\nabla \cdot E\|^2_{\varepsilon-1,\Omega_{t^*}} + \|E\|^2_{\sigma,\Omega_{t^*}}) \\ &= g(t^*) + C\int_0^{t^*} F(t)\,\mathrm{d}t \end{aligned}$$

for a constant $C > 0$, where

$$\begin{aligned} F(t) &:= \|\partial_t E\|^2_\varepsilon(t) + \|\nabla E\|^2(t) + \|\nabla \cdot E\|^2_{\varepsilon-1}(t) + \|E\|^2_\sigma(t), \\ g(t) &:= \|f_1\|^2_\varepsilon + \|\nabla f_0\|^2 + \|\nabla \cdot f_0\|^2_{\varepsilon-1} + 2\|f_0\|^2_\sigma + \int_0^{t^*} \|j\|^2\,\mathrm{d}t. \end{aligned}$$

An application of Grönwall's inequality yields (4.1). □

The next corollary follows from the stability estimate for the continuous problem, where all components of the electric field E are replaced with their approximations E_h, as well as all other continuous functions are replaced with their discrete analogs.

Corollary 4.1. *Assume that condition* (2.2) *on the functions* $\varepsilon(x), \sigma(x)$ *hold. For any* $t^* \in (0,T)$ *let* $\Omega_{t^*} = \Omega \times (0,t^*)$ *and* $\Gamma_{t^*} = \Gamma \times (0,t^*)$. *Suppose that there exists a solution* $E_h \in \mathbf{W}_h^E(\Omega)$ *of problem* (3.5) *and the approximations of the initial data* $f_{0,h}$ *and* $f_{1,h}$ *satisfy the regularity conditions* $f_{1,h}, f_{0,h} \in \mathbf{W}_h^E(\Omega)$. *Then* E_h *is unique and there exists a constant* $C = C(\|\varepsilon\|_{C^2(\Omega)}, \|\sigma\|, t^*)$ *such that the following energy estimate holds for all* $\varepsilon \geqslant 1, \sigma > 0, \varepsilon > \sigma$ *in* (3.5)*:*

$$
\begin{aligned}
(4.10) \qquad |\!|\!| E_h |\!|\!|^2(t^*) &:= \|\partial_t E_h\|_\varepsilon^2(t^*) + \|E_h\|_\sigma^2(t^*) + \|\nabla E_h\|^2(t^*) + \|\nabla \cdot E_h\|_{\varepsilon-1}^2(t^*) \\
&\leqslant C[\|j\|_{\Omega_{t^*}}^2 + \|f_{1,h}\|_\varepsilon^2 + \|\nabla f_{0,h}\|^2 + \|f_{0,h}\|_\sigma^2 + \|\nabla \cdot f_{0,h}\|_{\varepsilon-1}^2].
\end{aligned}
$$

5. A priori error estimates

In this section we present an *a priori error* estimate for the error $e = E(\cdot,t) - E_h(\cdot,t)$ between the solution E of the model problem (2.6) and solution E_h of the semi-discretized problem (3.5).

Let

$$
(5.1) \qquad e := E(\cdot,t) - E_h(\cdot,t) = E - \Pi_h E + \Pi_h E - E_h = \eta + \xi,
$$

where $\eta := E - \Pi_h E$, $\xi := \Pi_h E - E_h$. Here, $\Pi_h E\colon \mathbf{H}_E^1(\Omega_T) \to \mathbf{W}_{\mathbf{h}}^{\mathbf{E}}(\mathbf{\Omega_T})$ is an elliptic projection operator for $E \in H(\mathrm{div},\Omega)$, see details in [2], [22], such that for all $\mathbf{v} \in \mathbf{W}_h^E(\Omega)$

$$
(5.2) \qquad a(\Pi_h E, \mathbf{v}) = a(E, \mathbf{v}).
$$

The first part of the error, $\eta = E - \Pi_h E$, can be estimated as follows.

Theorem 5.1. *Let* $E \in \mathbf{H}_E^2(\Omega_T)$ *be the solution of the continuous problem* (2.6). *Then*

$$
(5.3) \qquad \|\eta\|_{L^2} \leqslant C_I(\tau^2 \|D_t^2 E\| + h^2 \|D_x^2 E\|), \quad \|\eta\|_{H^1} \leqslant C_I(\tau \|D_t^2 E\| + h \|D_x^2 E\|).
$$

For the semi-discretized problem (3.5) *these estimates reduce to:*

$$
(5.4) \qquad \|\eta\|_{L^2} \leqslant C_I h^2 \|D_x^2 E\|, \quad \|\eta\|_{H^1} \leqslant C_I h \|D_x^2 E\|.
$$

P r o o f. We observe that using (5.2) we can get for all $v \in \mathbf{W}_h^E(\Omega_T)$

$$\begin{aligned} \|\eta\|^2 &= \|E - \Pi_h E\|^2 = (E - \Pi_h E, E - \Pi_h E) \\ &= (E - \Pi_h E, E - v) + (E - \Pi_h E, v - \Pi_h E) \\ &= (E - \Pi_h E, E - v) \leqslant \|E - \Pi_h E\| \|E - v\|, \end{aligned} \tag{5.5}$$

and thus,

$$\|\eta\| = \|E - \Pi_h E\| \leqslant \|E - v\|. \tag{5.6}$$

Taking $v = E_h^I$ in (5.6), where E_h^I is nodal interpolant of E, and using standard interpolation error estimates [22], [30], [15] for the fully discrete scheme in space and time, we get

$$\|\eta\|_{L^2} \leqslant C_I(\tau^2 \|D_t^2 E\| + h^2 \|D_x^2 E\|), \quad \|\eta\|_{H^1} \leqslant C_I(\tau \|D_t^2 E\| + h \|D_x^2 E\|), \tag{5.7}$$

where C_I are interpolation constants. For semi-discretized problem (3.5); the terms with $D_t^2 E$ disappear and these estimates reduce to (5.4). □

In the proof of the a priori error estimate we use the constant C as a moderate constant, which is adjusted throughout the proof, as well as well-posedness of the bilinear form $a(\cdot, \cdot)$. Let us briefly sketch the proof of the well-posedness of $a(\cdot, \cdot)$. We refer to [4] for the full details of this proof.

Let us define the linear form as

$$\mathcal{L}(\mathbf{v}) := -(j, v). \tag{5.8}$$

We now can rewrite equation (3.5) as

$$(\varepsilon \partial_{tt} E_h, \mathbf{v}) + (\sigma \partial_t E_h, \mathbf{v}) + a(E_h, \mathbf{v}) = \mathcal{L}(\mathbf{v}). \tag{5.9}$$

Theorem 5.2 (well-posedness of $a(\cdot, \cdot)$)**.** *Assume that the following condition holds true:*

$$|\nabla \varepsilon| \leqslant \frac{1}{2} \min\Big(\frac{1}{2}, \varepsilon - 1\Big). \tag{5.10}$$

Let

$$\|\!| E_h |\!\|_a^2 := \|E_h\|_\varepsilon^2 + \|\nabla E_h\|^2 + \|\nabla \cdot E_h\|_{\varepsilon - 1}^2. \tag{5.11}$$

Then for all E_h and $\mathbf{v} \in \mathbf{W}_h^E(\Omega)$ the discrete bilinear form $a(\cdot, \cdot)$ is well-posed, or:

$$a(E_h, E_h) \geqslant \frac{1}{2} \|\!| E_h |\!\|_a^2 \qquad \textit{(coercivity of } a\textit{)}, \tag{5.12}$$

$$a(E_h, \mathbf{v}) \leqslant C_2 \|\!| E_h |\!\|_a \|\!| \mathbf{v} |\!\|_a \quad \textit{(continuity of } a\textit{)}, \tag{5.13}$$

$$|\mathcal{L}(\mathbf{v})| \leqslant C_3 \|\!| \mathbf{v} |\!\|_a \qquad \textit{(continuity of } \mathcal{L}\textit{)}, \tag{5.14}$$

where C_i, $i = 2, 3$, are positive constants.

P r o o f. We use a Lax-Milgram approach, or we will show that the discrete bilinear form $a(\cdot,\cdot)$ is coercive, and both $a(\cdot,\cdot)$ and $\mathcal{L}(\cdot)$ are continuous.

To prove the coercivity of $a(\cdot,\cdot)$ we choose $\mathbf{v} = E_h$ in (3.7) to get

$$
\begin{aligned}
(5.15)\quad a(E_h, E_h) &= (\nabla E_h, \nabla E_h) + (\nabla(\varepsilon - 1)E_h, \nabla \cdot E_h) + ((\varepsilon - 1)\nabla \cdot E_h, \nabla \cdot E_h) \\
&= \|\nabla E_h\|^2 + \|\nabla \cdot E_h\|^2_{\varepsilon - 1} + (\nabla(\varepsilon - 1)E_h, \nabla \cdot E_h).
\end{aligned}
$$

In (5.15) we have used the equality

$$
(5.16)\qquad (\nabla \cdot ((\varepsilon - 1)E_h), \nabla \cdot \mathbf{v}) = (\nabla(\varepsilon - 1)E_h + (\varepsilon - 1)\nabla \cdot E_h, \nabla \cdot \mathbf{v}).
$$

Since $\nabla(\varepsilon - 1) = \nabla\varepsilon$, we can use the following estimate derived in [4]:

$$
(5.17)\qquad \pm((\nabla\varepsilon)E_h, \nabla \cdot E_h) \geqslant -\frac{1}{2}\|E_h\|^2_{|\nabla\varepsilon|} - \frac{1}{2}\|\nabla \cdot E_h\|^2_{|\nabla\varepsilon|}.
$$

Using (5.17) and assumption (5.10), we obtain the coercivity of a:

$$
\begin{aligned}
(5.18)\quad a(E_h, E_h) &= \|\nabla E_h\|^2 + \|\nabla \cdot E_h\|^2_{\varepsilon - 1} + (\nabla(\varepsilon - 1)E_h, \nabla \cdot E_h) \\
&\geqslant \|\nabla E_h\|^2 + \|\nabla \cdot E_h\|^2_{\varepsilon - 1} - \frac{1}{2}\|E_h\|^2_{|\nabla\varepsilon|} - \frac{1}{2}\|\nabla \cdot E_h\|^2_{|\nabla\varepsilon|} \geqslant \frac{1}{2}|\!|\!| E_h |\!|\!|^2_a.
\end{aligned}
$$

To prove the continuity of $a(\cdot,\cdot)$, we use *Cauchy-Schwarz inequality* and estimate (5.17) to obtain for all $\mathbf{v} \in \mathbf{W}^E_h(\Omega)$:

$$
\begin{aligned}
(5.19)\quad a(E_h, \mathbf{v}) &= (\nabla E_h, \nabla \mathbf{v}) + (\nabla \cdot ((\varepsilon - 1)E_h), \nabla \cdot \mathbf{v}) \\
&= (\nabla E_h, \nabla \mathbf{v}) + ((\varepsilon - 1)\nabla \cdot E_h, \nabla \cdot \mathbf{v}) + ((\nabla\varepsilon)E_h, \nabla \cdot \mathbf{v}) \\
&\leqslant \|\nabla E_h\|\|\nabla \mathbf{v}\| + \|\nabla \cdot E_h\|_{\varepsilon - 1}\|\nabla \cdot \mathbf{v}\|_{\varepsilon - 1} \\
&\quad + \|E_h\|_{|\nabla\varepsilon|}\|\nabla \cdot \mathbf{v}\|_{|\nabla\varepsilon|} \leqslant C|\!|\!| E_h |\!|\!|_a \cdot |\!|\!| \mathbf{v} |\!|\!|_a.
\end{aligned}
$$

Finally, we can verify the continuity of $\mathcal{L}(\mathbf{v})$:

$$
(5.20)\qquad |\mathcal{L}(\mathbf{v})| = |(-j, \mathbf{v})| \leqslant \|j\|\|\mathbf{v}\| \leqslant \|j\||\!|\!| \mathbf{v} |\!|\!|.
$$

□

Theorem 5.3. *Let $E \in \mathbf{H}^2_E(\Omega_T)$ solve the continuous problem (2.6), and $E_h \in \mathbf{W}^E_h(\Omega_T)$ solve the semi-discretized problem (3.5). Assume that $E(t)$, $\partial_t E(t)$, $\partial_{tt} E(t) \in H^2(\Omega)$. Further assume that assumptions (2.2) and (5.10) on functions ε and σ hold true, as well as $f_0, f_1 \in [H^1(\Omega)]^3$, f_{0h}, f_{1h}, $j_h \in [W^E_h(\Omega)]^3$ and*

$j \in [L^2(\Omega_T)]^3$. Then there exists a constant $C(\varepsilon, \sigma)$ such that for all $t \in [0, T]$ the following a priori error estimates hold:

$$
\begin{aligned}
\|e(t)\| &= ||E(\cdot,t) - E_h(\cdot,t)|| \\
&\leqslant C_I h^2 \bigg(\|D_x^2 E\|_\Omega + 2 d_1 t \int_0^T (\|\partial_{ss} D_x^2 E\|_\Omega + \|\partial_s D_x^2 E\|_\Omega)\, \mathrm{d}s \bigg), \\
\|e(t)\|_{H^1} &= ||E(\cdot,t) - E_h(\cdot,t)||_{H^1} \\
&\leqslant C_I h \bigg(\|D_x^2 E\|_\Omega + 2 d_1 t \int_0^T (\|\partial_{ss} D_x^2 E\|_\Omega + \|\partial_s D_x^2 E\|_\Omega)\, \mathrm{d}s \bigg).
\end{aligned} \tag{5.21}
$$

P r o o f. Since η is estimated via standard interpolation error estimates (5.3), we begin to estimate ξ. We first note that for all $\mathbf{v} \in \mathbf{W}_h^E(\Omega)$

$$
\begin{aligned}
a(\Pi_h E, \mathbf{v}) = a(E, \mathbf{v}) = &- (j, \mathbf{v}) - (\varepsilon \partial_{tt} E, \mathbf{v}) - (\sigma \partial_t E, \mathbf{v}) + (\varepsilon \partial_{tt} \Pi_h E, \mathbf{v}) \\
&+ (\sigma \partial_t \Pi_h E, \mathbf{v}) - (\varepsilon \partial_{tt} \Pi_h E, \mathbf{v}) - (\sigma \partial_t \Pi_h E, \mathbf{v}).
\end{aligned} \tag{5.22}
$$

Using (5.1), the equation above can be written as

$$
(\varepsilon \partial_{tt} \Pi_h E, \mathbf{v}) + (\sigma \partial_t \Pi_h E, \mathbf{v}) + a(\Pi_h E, \mathbf{v}) = -(j, \mathbf{v}) - (\varepsilon \partial_{tt} \eta, \mathbf{v}) - (\sigma \partial_t \eta, \mathbf{v}). \tag{5.23}
$$

By subtracting the first equation of (3.5) from the expression above and letting $\mathbf{v} := \partial_t \xi$, we arrive at

$$
(\varepsilon \partial_{tt} \xi, \partial_t \xi) + (\sigma \partial_t \xi, \partial_t \xi) + a(\xi, \partial_t \xi) = -(\varepsilon \partial_{tt} \eta, \partial_t \xi) - (\sigma \partial_t \eta, \partial_t \xi). \tag{5.24}
$$

Note that for all $\mathbf{v} \in \mathbf{W}_h^E(\Omega)$

$$
a(\xi, \mathbf{v}) = a(\Pi_h E - E_h, \mathbf{v}) = a(E - E_h, \mathbf{v}) = 0,
$$

by the properties of Π_h and the Galerkin orthogonality. Using this we observe that in (5.24) the term $a(\xi, \partial_t \xi) = 0$. Thus, we can estimate a lower bound of the left-hand side of (5.24) as

$$
(\varepsilon \partial_{tt} \xi, \partial_t \xi) + (\sigma \partial_t \xi, \partial_t \xi) + a(\xi, \partial_t \xi) \geqslant (\varepsilon \partial_{tt} \xi, \partial_t \xi) = \frac{1}{2} \partial_t \|\varepsilon \partial_t \xi\|_\Omega^2 \geqslant \frac{1}{2} \partial_t \|\partial_t \xi\|_\Omega^2, \tag{5.25}
$$

where we have used that $(\sigma \partial_t \xi, \partial_t \xi) \geqslant 0$ and $\varepsilon \geqslant 1, \sigma \geqslant 0$.

We can also estimate an upper bound for the right-hand side of (5.24):

$$
-(\varepsilon \partial_{tt} \eta, \partial_t \xi) - (\sigma \partial_t \eta, \partial_t \xi) \leqslant (\|\varepsilon \partial_{tt} \eta\|_\Omega + \|\sigma \partial_t \eta\|_\Omega) \|\partial_t \xi\|_\Omega. \tag{5.26}
$$

Collecting these two estimates, we have

$$
\partial_t \|\partial_t \xi\|_\Omega^2 \leqslant 2(\|\varepsilon \partial_{tt} \eta\|_\Omega + \|\sigma \partial_t \eta\|_\Omega) \|\partial_t \xi\|_\Omega. \tag{5.27}
$$

Integrating over $[0, t^*]$, where $t^* \in [0, T]$, using conditions (2.2) for functions ε, σ and noting that $\varepsilon > \sigma$, we get

$$\|\partial_t \xi\|_\Omega^2(t^*) \leqslant 2 \int_0^{t^*} (\|\varepsilon \partial_{ss}\eta\|_\Omega + \|\sigma \partial_s \eta\|_\Omega) \|\partial_s \xi\|_\Omega(s)\,\mathrm{d}s \tag{5.28}$$
$$\leqslant 2d_1 \int_0^{t^*} (\|\partial_{ss}\eta\|_\Omega + \|\partial_s \eta\|_\Omega)(s)\,\mathrm{d}s \cdot \max_{t' \in [0,T]} \|\partial_s \xi\|_\Omega,$$

where we have used that $\xi(\cdot, 0) = \partial_t \xi(\cdot, 0) = 0$, and $\sigma \leqslant \varepsilon \leqslant d_1$.

Since (5.28) holds for all $t^* \in [0, T]$, we have

$$\max_{t' \in [0,T]} \|\partial_t \xi\|_\Omega^2 \leqslant 2d_1 \int_0^T (\|\partial_{ss}\eta\|_\Omega + \|\partial_s \eta\|_\Omega)(s)\,\mathrm{d}s \cdot \max_{t' \in [0,T]} \|\partial_t \xi\|_\Omega, \tag{5.29}$$
$$\max_{t' \in [0,T]} \|\partial_t \xi\|_\Omega \leqslant 2d_1 \int_0^T (\|\partial_{ss}\eta\|_\Omega + \|\partial_s \eta\|_\Omega)(s)\,\mathrm{d}s.$$

Substituting this estimate into (5.28), we finally obtain

$$\|\partial_t \xi\|_\Omega \leqslant 2d_1 \int_0^T (\|\partial_{ss}\eta\|_\Omega + \|\partial_s \eta\|_\Omega)(s)\,\mathrm{d}s. \tag{5.30}$$

To proceed further we use estimate (5.3) to get

$$\int_0^{t^*} (\|\partial_{ss}\eta\|_\Omega + \|\partial_s \eta\|_\Omega)(s)\,\mathrm{d}s \leqslant C_I h^2 \int_0^T (\|\partial_{ss} D_x^2 E\|_\Omega + \|\partial_s D_x^2 E\|_\Omega)\,\mathrm{d}s. \tag{5.31}$$

Using (5.31) in (5.30) we obtain

$$\|\partial_t \xi\|_\Omega \leqslant 2d_1 C_I h^2 \int_0^T (\|\partial_{ss} D_x^2 E\|_\Omega + \|\partial_s D_x^2 E\|_\Omega)\,\mathrm{d}s. \tag{5.32}$$

Further, we observe that

$$\frac{\mathrm{d}}{\mathrm{dt}} \|\xi\|_\Omega^2 = 2\|\xi\|_\Omega \frac{\mathrm{d}}{\mathrm{dt}} \|\xi\|_\Omega = \frac{\mathrm{d}}{\mathrm{dt}} \int_\Omega |\xi|^2\,\mathrm{d}x = 2 \int_\Omega \xi \cdot \xi_t\,\mathrm{d}x \leqslant 2\|\xi\|_\Omega \|\partial_t \xi\|_\Omega, \tag{5.33}$$

from which it follows that

$$\frac{\mathrm{d}}{\mathrm{dt}} \|\xi\|_\Omega \leqslant \|\partial_t \xi\|_\Omega. \tag{5.34}$$

Integrating in time (5.34) and using (5.32) yields

$$\|\xi(t)\|_\Omega \leqslant \int_0^t \|\partial_s \xi\|_\Omega\,\mathrm{d}s \leqslant 2d_1 C_I h^2 t \int_0^T (\|\partial_{ss} D_x^2 E\|_\Omega + \|\partial_s D_x^2 E\|_\Omega)\,\mathrm{d}s. \tag{5.35}$$

From (5.35) and (5.3) it follows also that

$$\|\xi(t)\|_{H^1} \leqslant 2d_1 C_I ht \int_0^T (\|\partial_{ss} D_x^2 E\|_\Omega + \|\partial_s D_x^2 E\|_\Omega)\,\mathrm{d}s. \tag{5.36}$$

Summing up (5.3), (5.35) and (5.36) we get the desired error estimates (5.21), and the proof is complete. □

6. Numerical examples

In this section we perform computations which will confirm theoretical predictions given in Theorem 5.3. All computations are performed in the software package WavES [9] using C++/PETSc [6]. The computational domain $\Omega \times (0,T)$ is chosen as $\Omega = [0,1] \times [0,1]$ with $\Omega_1 = [0.25, 0.75] \times [0.25, 0.75]$ such that $\Omega_1 \subset \Omega$. To discretize the computational domain Ω we denote by $\mathcal{T}_{hl} := \{K\}$ a partition of the domain $\overline{\Omega}$ into triangles K of sizes $h_l = 2^{-l}$, $l = 3, \ldots, 6$. The explicit finite element scheme (3.9) derived in [11] was used in computations. We have chosen the time step $\tau = 0.0005$ such that the whole explicit scheme remains stable.

We have used the following time-dependent model problem in computations:

$$\begin{aligned} &\varepsilon(\mathbf{x})\frac{\partial^2 E(\mathbf{x},t)}{\partial t^2} + \nabla \times \nabla \times E(\mathbf{x},t) + \sigma(\mathbf{x})\frac{\partial E(\mathbf{x},t)}{\partial t} = f(\mathbf{x},t), \\ &\nabla \cdot (\varepsilon E)(\mathbf{x},t) = 0, \quad E(\mathbf{x},0) = 0, \quad \frac{\partial E}{\partial t}(\mathbf{x},0) = 0, \quad E|_\Gamma = 0. \end{aligned} \tag{6.1}$$

The source data $f(\mathbf{x},t)$, $\mathbf{x} := (x,y) \in \mathbb{R}^2$, $t \in [0, 0.25]$, is computed by knowing the exact solution

$$E_1(\mathbf{x},t) = \frac{t^2}{\varepsilon}\pi \sin^2 \pi x \cos \pi y \sin \pi y, \quad E_2(\mathbf{x},t) = -\frac{t^2}{\varepsilon}\pi \sin^2 \pi y \cos \pi x \sin \pi x \tag{6.2}$$

of problem (6.1).

In the model problem (6.1), the function $\varepsilon(x,y)$ is defined as

$$\varepsilon(x,y) = \begin{cases} 1 + (\sin \pi(2x - 0.375))^m \cdot (\sin \pi(2y - 0.375))^m \\ \quad + (\sin \pi(2x - 0.625))^m \cdot (\sin \pi(2y - 0.625))^m & \text{in } \Omega_1, \\ 1 & \text{otherwise,} \end{cases} \tag{6.3}$$

and the function $\sigma(x,y)$ as

$$\sigma(x,y) = \begin{cases} 0.001(1 + (\sin \pi(2x - 0.375))^m \cdot (\sin \pi(2y - 0.375))^m \\ \quad + (\sin \pi(2x - 0.625))^m \cdot (\sin \pi(2y - 0.625))^m) & \text{in } \Omega_1, \\ 0 & \text{otherwise.} \end{cases} \tag{6.4}$$

Figures 2, 3 show the functions ε and σ, respectively, for different $m = 6, 8, 10, 12$ in (6.3), (6.4), which were used in computations.

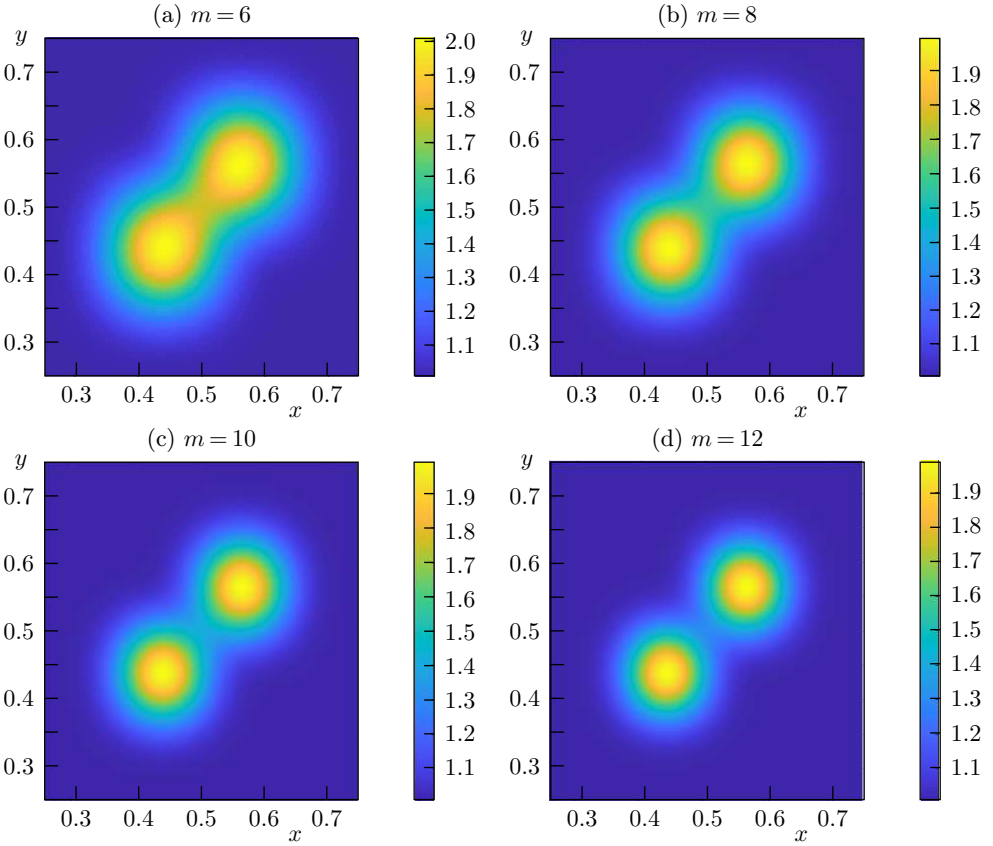


Figure 2. The function $\varepsilon(x, y)$ in the domain $\Omega_1 = [0.25, 0.75] \times [0.25, 0.75]$ for different values of m in (6.3).

Relative errors $\Theta^{(1)}$, $\Theta^{(2)}$ are computed at the time moment $t = 0.25$ as

$$\Theta^{(1)} = \frac{\|\widehat{E} - \widehat{E}_h\|_{L^2}}{\|\widehat{E}\|_{L^2}} \tag{6.5}$$

and

$$\Theta^{(2)} = \frac{\|\nabla(\widehat{E} - \widehat{E}_h)\|_{L^2}}{\|\nabla\widehat{E}\|_{L^2}}, \tag{6.6}$$

in L^2- and H^1-norms, respectively. Here, $\widehat{E} = (\widehat{E}_1, \widehat{E}_2)$ is the exact solution given by (6.2), and $\widehat{E}_h = (\widehat{E}_{1h}, \widehat{E}_{2h})$ is the computed solution. We also note that

$$|\widehat{E}| := \sqrt{\widehat{E}_1^2 + \widehat{E}_2^2}, \quad |\widehat{E}_h| := \sqrt{\widehat{E}_{1h}^2 + \widehat{E}_{2h}^2}. \tag{6.7}$$

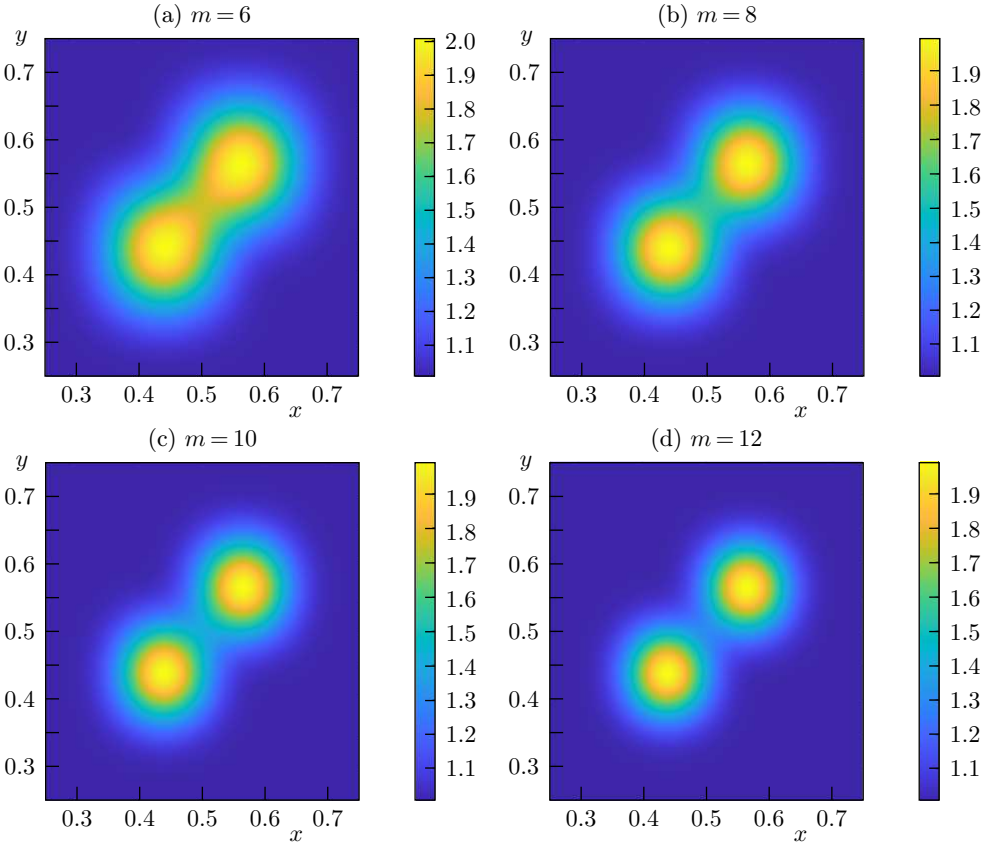


Figure 3. The function $\sigma(x, y)$ in the domain $\Omega_1 = [0.25, 0.75] \times [0.25, 0.75]$ for different values of m in (6.3).

Figure 4 present convergence results of explicit finite element scheme (3.9) for the functions ε and σ defined by (6.3), (6.4), respectively, for different values of $m = 6, 8, 10, 12$. Table 1–4 present relative errors $\Theta_l^{(j)}$, $j = 1, 2$ and convergence rates $r_l^{(j)}$, $j = 1, 2$ in the L^2-norm and in the H^1-norm for mesh sizes $h_l = 2^{-l}$, $l = 3, \ldots, 6$, for different values of $m = 6, 8, 10, 12$ in (6.3) and (6.4). We note that chosen values of m satisfy the regularity assumptions on the exact solution, see details in [13].

We used the following expressions to compute convergence rates $r^{(1)}$ and $r^{(2)}$ presented in these figures and tables:

$$r^{(1)} = \frac{1}{|\log 2|}\left|\log\frac{\Theta_l^{(1)}}{\Theta_{l+1}^{(1)}}\right|, \quad r^{(2)} = \frac{1}{|\log 2|}\left|\log\frac{\Theta_l^{(2)}}{\Theta_{l+1}^{(2)}}\right|, \tag{6.8}$$

where $\Theta_l^{(j)}$, $j = 1, 2$, are computed relative norms $\Theta^{(j)}$, $j = 1, 2$, on the mesh $\mathcal{T}_h$ with the mesh sizes $h_l = 2^{-l}$, $l = 3, \ldots, 5$.

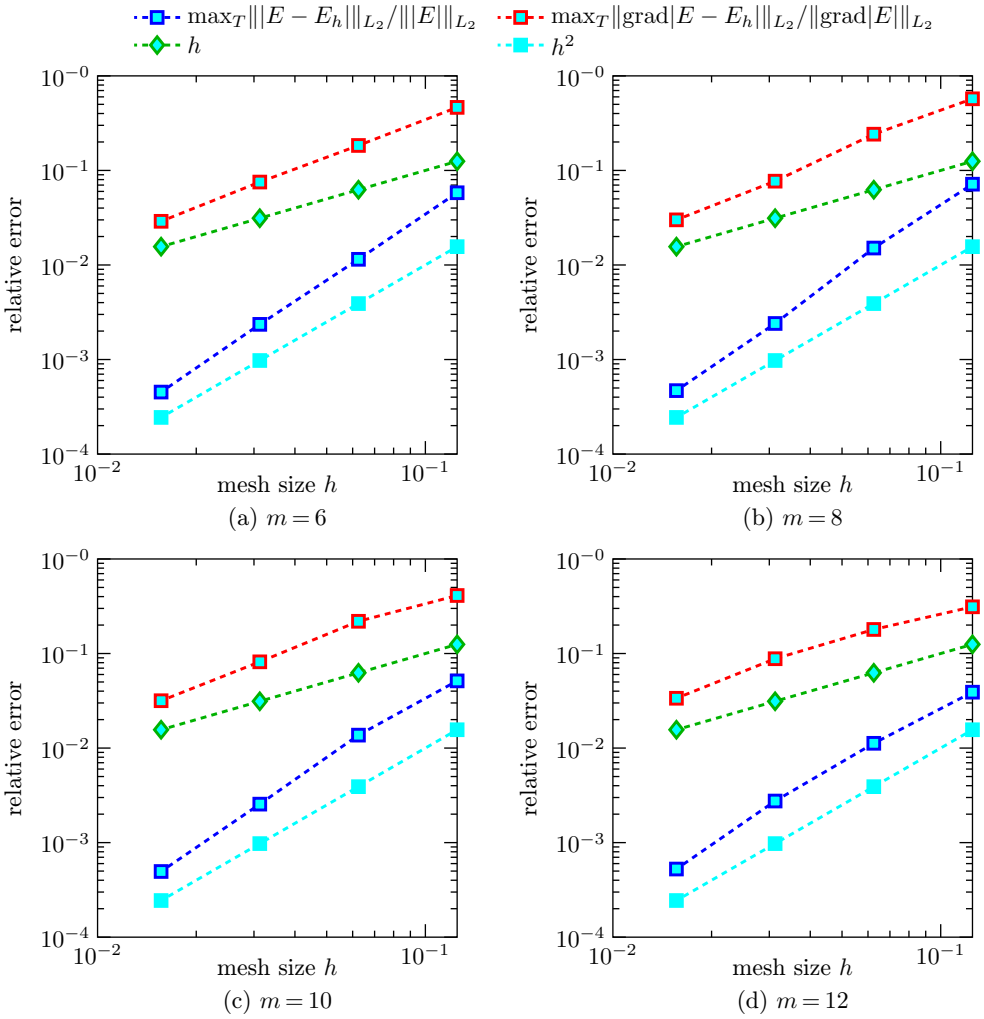


Figure 4. Relative errors for different m in (6.3) and (6.4).

l	nel	nno	$\Theta^{(1)}$	$\frac{\Theta_l^{(1)}}{\Theta_{l+1}^{(1)}}$	$r^{(1)}$	$\Theta^{(2)}$	$\frac{\Theta_l^{(2)}}{\Theta_{l+1}^{(2)}}$	$r^{(2)}$
3	128	81	0.058066	-	-	0.464524	-	-
4	512	289	0.011481	5.057543	2.34	0.183696	2.528771	1.34
5	2048	1089	0.002355	4.875048	2.29	0.075362	2.437524	1.29
6	8192	4225	0.000453	5.202624	2.38	0.028971	2.601312	1.38

Table 1. Relative errors $\Theta_l^{(j)}$, $j = 1, 2$ and convergence rates $r_l^{(j)}$, $j = 1, 2$, in the L^2-norm and in the H^1-norm for mesh sizes $h_l = 2^{-l}$, $l = 3, \ldots, 6$, for $m = 6$ in (6.3) and (6.4).

l	nel	nno	$\Theta^{(1)}$	$\frac{\Theta_l^{(1)}}{\Theta_{l+1}^{(1)}}$	$r^{(1)}$	$\Theta^{(2)}$	$\frac{\Theta_l^{(2)}}{\Theta_{l+1}^{(2)}}$	$r^{(2)}$
3	128	81	0.071545	-	-	0.572362	-	-
4	512	289	0.015110	4.735050	2.24	0.241756	2.367525	1.24
5	2048	1089	0.002406	6.280222	2.65	0.076989	3.140111	1.65
6	8192	4225	0.000469	5.130590	2.36	0.030012	2.565295	1.36

Table 2. Relative errors $\Theta_l^{(j)}$, $j = 1, 2$ and convergence rates $r_l^{(j)}$, $j = 1, 2$, in the L^2-norm and in the H^1-norm for mesh sizes $h_l = 2^{-l}$, $l = 3, \ldots, 6$, for $m = 8$ in (6.3) and (6.4).

l	nel	nno	$\Theta^{(1)}$	$\frac{\Theta_l^{(1)}}{\Theta_{l+1}^{(1)}}$	$r^{(1)}$	$\Theta^{(2)}$	$\frac{\Theta_l^{(2)}}{\Theta_{l+1}^{(2)}}$	$r^{(2)}$
3	128	81	0.051348	-	-	0.410785	-	-
4	512	289	0.013703	3.747278	1.91	0.219245	1.873639	0.91
5	2048	1089	0.002553	5.367863	2.42	0.081688	2.683932	1.42
6	8192	4225	0.000495	5.156936	2.37	0.031681	2.578468	1.37

Table 3. Relative errors $\Theta_l^{(j)}$, $j = 1, 2$ and convergence rates $r_l^{(j)}$, $j = 1, 2$, in the L^2-norm and in the H^1-norm for mesh sizes $h_l = 2^{-l}$, $l = 3, \ldots, 6$, for $m = 10$ in (6.3) and (6.4).

l	nel	nno	$\Theta^{(1)}$	$\frac{\Theta_l^{(1)}}{\Theta_{l+1}^{(1)}}$	$r^{(1)}$	$\Theta^{(2)}$	$\frac{\Theta_l^{(2)}}{\Theta_{l+1}^{(2)}}$	$r^{(2)}$
3	128	81	0.038995	-	-	0.311959	-	-
4	512	289	0.011230	3.472240	1.80	0.179688	1.736128	0.80
5	2048	1089	0.002753	4.078874	2.03	0.088106	2.039437	1.03
6	8192	4225	0.000526	5.238828	2.39	0.033636	2.619414	1.39

Table 4. Relative errors $\Theta_l^{(j)}$, $j = 1, 2$ and convergence rates $r_l^{(j)}$, $j = 1, 2$, in the L^2-norm and in the H^1-norm for mesh sizes $h_l = 2^{-l}$, $l = 3, \ldots, 6$, for $m = 12$ in (6.3) and (6.4).

Using Figure 4 and Tables 1–4 we observe that the explicit finite element scheme derived in [11] behaves like a first order method in $H^1(\Omega)$-norm and second order method in $L^2(\Omega)$-norm. Therefore, these results confirm theoretical analytic estimates derived in Theorem 5.3.

7. Conclusions

This paper presents stability and convergence analysis for the finite element method for stabilized time-dependent Maxwell's equations in conductive nonmagnetic media developed in [11]. We present the analysis for a specific case when the dielectric permittivity and conductivity functions have a constant value in a boundary neighborhood.

In the theoretical part of the paper we derived energy norm stability estimates for the continuous and discrete solutions of the model problem, as well as a priori error bounds in the gradient dependent, weighted norms. Our numerical computations confirm theoretical predictions and show that our method behaves like a first order method in $H^1(\Omega)$-norm and second order method in $L^2(\Omega)$-norm.

Open Access. This article is licensed under a Creative Commons Attribution 4.0 International License, which permits use, sharing, adaptation, distribution and reproduction in any medium or format, as long as you give appropriate credit to the original author(s) and the source, provide a link to the Creative Commons licence, and indicate if changes were made. The images or other third party material in this article are included in the article's Creative Commons licence, unless indicated otherwise in a credit line to the material. If material is not included in the article's Creative Commons licence and your intended use is not permitted by statutory regulation or exceeds the permitted use, you will need to obtain permission directly from the copyright holder. To view a copy of this licence, visit `http://creativecommons.org/licenses/by/4.0/`.

References

[1] *D. N. Arnold, F. Brezzi, B. Cockburn, L. D. Marini*: Unified analysis for discontinuous Galerkin methods for elliptic problems. SIAM J. Numer. Anal. *39* (2022), 1749–1779. zbl MR doi

[2] *M. Asadzadeh*: An Introduction to Finite Element Methods for Differential Equations. John Wiley & Sons, Hoboken, 2021. zbl doi

[3] *M. Asadzadeh, L. Beilina*: Stability and convergence analysis of a domain decomposition FE/FD method for Maxwell's equations in the time domain. Algorithms *15* (2022), Article ID 337, 22 pages. doi

[4] *M. Asadzadeh, L. Beilina*: A stabilized $P1$ domain decomposition finite element method for time harmonic Maxwell's equations. Math. Comput. Simul. *204* (2023), 556–574. zbl MR doi

[5] *F. Assous, P. Degond, E. Heinze, P. A. Raviart, J. Segre*: On finite-element method for solving the three-dimensional Maxwell equations. J. Comput. Phys. *109* (1993), 222–237. zbl MR doi

[6] *S. Balay, W. D. Gropp, L. C. McInnes, B. F. Smith*: PETSc: The Portable, Extensible Toolkit for Scientific Computation. Available at `http://www.mcs.anl.gov/petsc/`. sw

[7] *L. Baudouin, M. de Buhan, S. Ervedoza, A. Osses*: Carleman-based reconstruction algorithm for the waves. SIAM J. Numer. Anal. *59* (2021), 998–1039. zbl MR doi

[8] *L. Beilina*: Energy estimates and numerical verification of the stabilized domain decomposition finite element/finite difference approach for time-dependent Maxwell's system. Cent. Eur. J. Math. *11* (2013), 702–733. zbl MR doi
[9] *L. Beilina*: WavES: Wave Equations Solutions. Available at `http://www.waves24.com/` (2017). sw
[10] *L. Beilina, M. V. Klibanov*: Approximate Global Convergence and Adaptivity for Coefficient Inverse Problems. Springer, New York, 2012. zbl doi
[11] *L. Beilina, E. Lindström*: An adaptive finite element/finite difference domain decomposition method for applications in microwave imaging. Electronics *11* (2022), Article ID 1359, 33 pages. doi
[12] *L. Beilina, E. Lindström*: A posteriori error estimates and adaptive error control for permittivity reconstruction in conductive media. Gas Dynamics with Applications in Industry and Life Sciences. Springer Proceedings in Mathematics & Statistics 429. Springer, Cham, 2023, pp. 117–141. MR doi
[13] *L. Beilina, V. Ruas*: An explicit P1 finite element scheme for Maxwell's equations with constant permittivity in a boundary neighborhood. Available at `https://arxiv.org/abs/1808.10720` (2018), 38 pages. doi
[14] *A.-S. Bonnet-Ben Dhia, C. Hazard, S. Lohrengel*: A singular field method for the solution of Maxwell's equations in polyhedral domains. SIAM J. Appl. Math. *59* (1999), 2028–2044. zbl MR doi
[15] *S. C. Brenner, L. R. Scott*: The Mathematical Theory of Finite Element Methods. Texts in Applied Mathematics 15. Springer, New York, 1994. zbl MR doi
[16] *P. Ciarlet,* Jr.: Augmented formulations for solving Maxwell equations. Comput. Methods Appl. Mech. Eng. *194* (2005), 559–586. zbl MR doi
[17] *P. Ciarlet,* Jr., *E. Jamelot*: Continuous Galerkin methods for solving the time-dependent Maxwell equations in 3D geometries. J. Comput. Phys. *226* (2007), 1122–1135. zbl MR doi
[18] *G. C. Cohen*: Higher-Order Numerical Methods for Transient Wave Equations. Scientific Computation. Springer, Berlin, 2002. zbl MR doi
[19] *M. Costabel, M. Dauge*: Singularities of electromagnetic fields in polyhedral domains. Arch. Ration. Mech. Anal. *151* (2000), 221–276. zbl MR doi
[20] *M. Costabel, M. Dauge*: Weighted regularization of Maxwell equations in polyhedral domains: A rehabilitation of nodal finite elements. Numer. Math. *93* (2002), 239–277. zbl MR doi
[21] *A. Elmkies, P. Joly*: Edge finite elements and mass lumping for Maxwell's equations: The 2D case. C. R. Acad. Sci., Paris, Sér. I *324* (1997), 1287–1293. (In French.) zbl MR doi
[22] *K. Eriksson, D. Estep, P. Hansbo, C. Johnson*: Computational Differential Equations. Cambridge University Press, Cambridge, 1996. zbl MR
[23] *A. Ern, J.-L. Guermond*: Analysis of the edge finite element approximation of the Maxwell equations with low regularity solutions. Comput. Math. Appl. *75* (2018), 918–932. zbl MR doi
[24] *L. C. Evans*: Partial Differential Equations. Graduate Studies in Mathematics 19. AMS, Providence, 1998. zbl MR doi
[25] *Y. G. Gleichmann, M. J. Grote*: Adaptive spectral inversion for inverse medium problems. Inverse Probl. *39* (2023), Article ID 125007, 27 pages. zbl MR doi
[26] *E. Jamelot*: Résolution des équations de Maxwell avec des éléments finis de Galerkin continus: PhD Thesis. L'Ecole Polytechnique, Paris, 2005. (In French.) zbl
[27] *B.-n. Jiang*: The Least-Squares Finite Element Method: Theory and Applications in Computational Fluid Dynamics and Electromagnetics. Scientific Computation. Springer, Berlin, 1998. zbl MR doi
[28] *B.-n. Jiang, J. Wu, L. A. Povinelli*: The origin of spurious solutions in computational electromagnetics. J. Comput. Phys. *125* (1996), 104–123. zbl MR doi

[29] *J.-M. Jin*: The Finite Element Method in Electromagnetics. John Wiley, New York, 1993. zbl MR
[30] *C. Johnson*: Numerical Solutions of Partial Differential Equations by the Finite Element Method. Cambridge University Press, Cambridge, 1987. zbl MR
[31] *P. Joly*: Variational methods for time-dependent wave propagation problems. Topics in Computational Wave Propagation. Lecture Notes in Computational Science and Engineering 31. Springer, Berlin, 2003, pp. 201–264. zbl MR doi
[32] *M. Křížek, P. Neittaanmäki*: Finite Element Approximation of Variational Problems and Applications. Pitman Monographs and Surveys in Pure and Applied Mathematics 50. Longman, Harlow, 1990. zbl MR
[33] *M. Křížek, P. Neittaanmäki*: Mathematical and Numerical Modelling in Electrical Engineering: Theory and Applications. Kluwer Academic, Dordrecht, 1996. zbl MR doi
[34] *M. Lazebnik,* et al.: A large-scale study of the ultrawideband microwave dielectric properties of normal, benign and malignant breast tissues obtained from cancer surgeries. Phys. Med. Biol. *52* (2007), Article ID 6093, 20 pages. doi
[35] *J. B. Malmberg, L. Beilina*: An adaptive finite element method in quantitative reconstruction of small inclusions from limited observations. Appl. Math. Inf. Sci. *12* (2018), 1–19. MR doi
[36] *P. Monk*: Finite Element Methods for Maxwell's Equations. Numerical Mathematics and Scientific Computation. Oxford University Press, Oxford, 2003. zbl MR doi
[37] *P. B. Monk, A. K. Parrott*: A dispersion analysis of finite element methods for Maxwell's equations. SIAM J. Sci. Comput. *15* (1994), 916–937. zbl MR doi
[38] *C.-D. Munz, P. Omnes, R. Schneider, E. Sonnendrücker, U. Voss*: Divergence correction techniques for Maxwell solvers based on a hyperbolic model. J. Comput. Phys. *161* (2000), 484–511. zbl MR doi
[39] *J.-C. Nedelec*: Mixed finite elements in $\mathbb{R}^3$. Numer. Math. *35* (1980), 315–341. zbl MR doi
[40] *K. D. Paulsen, D. R. Lynch*: Elimination of vector parasites in finite element Maxwell solutions. IEEE Trans. Microw. Theory Tech. *39* (1991), 395–404. doi
[41] *N. T. Thành, L. Beilina, M. V. Klibanov, M. A. Fiddy*: Reconstruction of the refractive index from experimental backscattering data using a globally convergent inverse method. SIAM J. Sci. Comput. *36* (2014), B273–B293. zbl MR doi
[42] *N. T. Thành, L. Beilina, M. V. Klibanov, M. A. Fiddy*: Imaging of buried objects from experimental backscattering time-dependent measurements using a globally convergent inverse algorithm. SIAM J. Imaging Sci. *8* (2015), 757–786. zbl MR doi

Authors' address: *Eric Lindström*, *Larisa Beilina* (corresponding author), Department of Mathematical Sciences, Chalmers University of Technology and Gothenburg University, SE-42196 Gothenburg, Sweden, e-mail: `erilinds@chalmers.se`, `larisa@chalmers.se`.